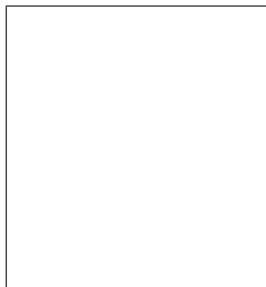


## B Physics at CDF

Jonas Rademacker  
 on behalf of the CDF Collaboration  
*Department of Physics, 1 Keble Road,  
 Oxford OX1 3RH, UK*



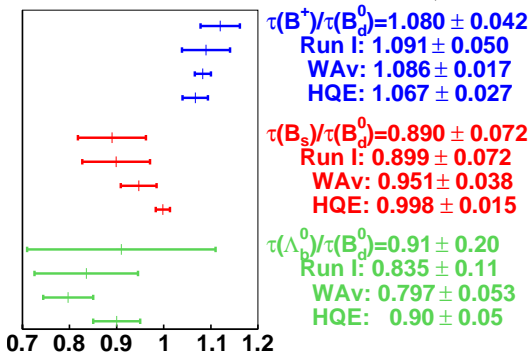
Due to the large  $b\bar{b}$  cross section at 1.96 TeV  $p - \bar{p}$  collisions, the Tevatron is currently the most copious source of B hadrons. Recent detector upgrades for Run II have made these more accessible, allowing for a wide range of B and  $\mathcal{CP}$  physics with B hadrons of all flavours. In this paper we present B-physics results, and, using the versatile hadronic Two Track Trigger, a search for  $\Xi(1860)$ , from up to  $240 \text{ pb}^{-1}$  of data.

### 1 Introduction

CDF has been taking data at Tevatron Run IIa for about two years. For  $p\bar{p}$  collisions at 1.96 TeV, the  $b\bar{b}$  production cross section is  $\sigma_{b\bar{b}} \sim 0.1 \text{ mb}$ . CDF has undergone major upgrades for Run II, optimising its B physics potential. The upgrades most relevant for CDF's B physics program include a new tracking system with a new, faster drift chamber, and new Silicon vertex trackers providing excellent proper time resolution, sufficient to resolve the expected fast oscillations in the  $B_s^0$  system. The excellent impact parameter resolution is used for triggering on B-events. The muon coverage has been increased. A di-muon trigger efficiently finds  $B \rightarrow J/\psi X$  decays.

Here we present some of the wide range of analyses of the current CDF B physics program, which includes a wide range of studies, involving all types of B-hadrons, including leptonic as well as fully hadronic decays of  $B_d, B^+, B_s, B_c, \Lambda_b$ . The impact-parameter based trigger also provides a very large sample of long-lived  $\Xi^-$ . This has been used for a sensitive search for  $\Xi^0(1860) \rightarrow \Xi^- \pi^+$  and  $\Xi^{--} \rightarrow \Xi^- \pi^-$ , which have been observed at NA49<sup>1</sup> and are often interpreted as pentaquark states.

Table 1: Lifetimes and lifetime ratios in Run II from  $B_u^+ \rightarrow J/\psi(\mu^+\mu^-)K^+$  ( $240 \text{ pb}^{-1}$ ),  $B_d^0 \rightarrow J/\psi(\mu^+\mu^-)K^{(*)0}$  ( $240 \text{ pb}^{-1}$ ),  $B_s^0 \rightarrow J/\psi(\mu^+\mu^-)\phi$  ( $240 \text{ pb}^{-1}$ ),  $\Lambda_b \rightarrow J/\psi(\mu^+\mu^-)\Lambda$  ( $65 \text{ pb}^{-1}$ ) compared with world average (HFAG<sup>4</sup>, results for PDG 04, and, for  $\Lambda_b$ , results for PDG 02), Run I results<sup>5</sup> and HQE predictions<sup>6</sup>. Run I results are from all channels combined, Run II results from fully reconstructed  $J/\psi(\mu\mu)X$  only.



Channel	Result (ps)
$B_u^+ \rightarrow J/\psi(\mu^+\mu^-)K^+$	$1.662 \pm 0.022 \pm 0.008$
$B_d^0 \rightarrow J/\psi(\mu^+\mu^-)K^{(*)0}$	$1.539 \pm 0.051 \pm 0.008$
$B_s^0 \rightarrow J/\psi(\mu^+\mu^-)\phi$	$1.369 \pm 0.100^{+0.008}_{-0.010}$
$\Lambda_b^0 \rightarrow J/\psi(\mu^+\mu^-)\Lambda$	$1.25 \pm 0.25 \pm 0.10$

Note that the Run II result for  $B_s \rightarrow J/\psi\phi$  is dominated by the (shorter) lifetime of the CP-even component.

## 2 Results from the Di-Muon Trigger

### 2.1 $b$ Production Cross Section

The inclusive  $b$ -hadron production cross-section is measured from the  $b$ -fraction in the reconstructed  $J/\psi$  sample up to February 2002 ( $37 \text{ pb}^{-1}$ ). Combining this number with the inclusive  $J/\psi X$  cross section, and the appropriate branching fractions, allows to calculate the absolute  $b$  production cross section. The long lifetime of B-hadrons is used to discriminate between prompt  $J/\psi$  and  $J/\psi$  from B-hadron decays. The total single  $b$ -quark cross-section integrated over one unit of rapidity is

$$\sigma(p\bar{p} \rightarrow \bar{b}X : |y| < 1.0) = 29.4 \pm 0.6(\text{stat}) \pm 6.2(\text{sys}) \mu\text{b}$$

where the largest contributions to the systematic error come from uncertainties in the acceptance and the inclusive B-hadron to  $J/\psi$  branching ratio.

### 2.2 Lifetimes

Life time measurements in the heavy quark sector gain specific significance due to the precise predictions of Heavy Quark Expansion<sup>23</sup> thus providing a testing ground for this theoretical tool that is frequently used, for example to relate experimental measurements to CKM parameters like  $\Gamma_d$  to  $|V_{cb}|$  or  $\Delta m_s/\Delta m_d$  to  $|V_{ts}/V_{td}|$ .

Fully reconstructed hadronic  $B \rightarrow J/\psi X$  decays, found with CDF's di-muon trigger, provide a clean method for measuring B lifetimes, free from the systematic uncertainties associated with semileptonic decays due to the missing momentum of the  $\nu$ , and free from the lifetime bias in impact parameter-based trigger samples. Of specific interest at CDF are the lifetimes of the  $B_s$  and  $\Lambda_b$ , which are currently produced in large quantities only at the Tevatron. Lifetime results, and lifetime ratios, compared to theory predictions, Run I results, and world averages, are summarised in Table 1.

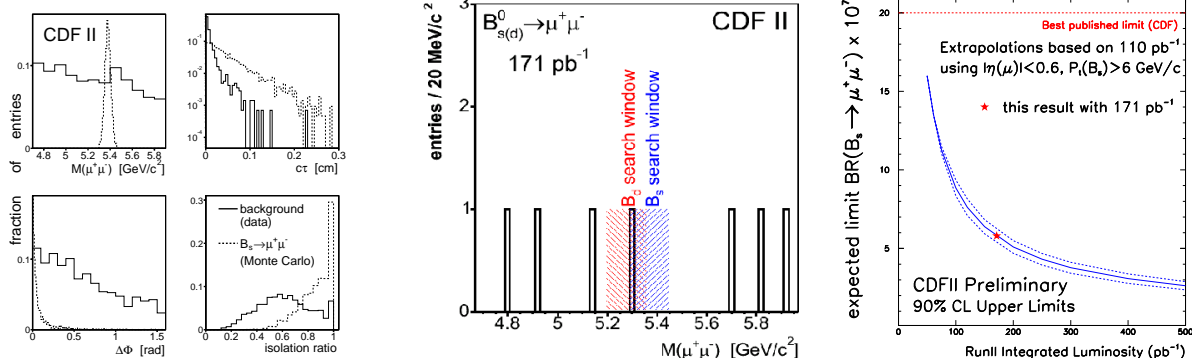
### 2.3 CP content of $B_s \rightarrow J/\psi\phi$

The measurement of the average lifetime in  $B_s \rightarrow J/\psi\phi$  constitutes a first step towards a measurement of  $\Delta\Gamma_s$ , the width difference between the long and short lived CP eigenstates, which has some sensitivity to new physics, especially when compared to the mass difference,  $\Delta m_s$ , which is also going to be measured at the Tevatron. The CP-even and odd contribution in  $B_s \rightarrow J/\psi\phi$  can be disentangled by analysing the decay in terms of transversity angles, leading

Table 2: Transversity-angle analysis in  $B_s \rightarrow J/\psi\phi$  and  $B_d \rightarrow J/\psi K^{*0}$ .  $A_0$  and  $A_{\parallel}$  are CP even decay amplitudes,  $A_{\perp}$  is CP-odd, normalised such that  $|A_0|^2 + |A_{\parallel}|^2 + |A_{\perp}|^2 \equiv 1$ .

$B_s \rightarrow J/\psi\phi$	$B_d \rightarrow J/\psi K^{*0}$
$A_0 = 0.762 \pm 0.044 \pm 0.07$	$A_0 = 0.796 \pm 0.022 \pm 0.012$
$A_{\parallel} = (0.433 \pm 0.199 \pm 0.011) e^{i(2.08 \pm 0.51 \pm 0.06)}$	$A_{\parallel} = (0.433 \pm 0.037 \pm 0.014) e^{i(3.10 \pm 0.50 \pm 0.06)}$
$ A_{\perp}  = 0.481 \pm 0.104 \pm 0.025$	$A_{\perp} = (0.422 \pm 0.050 \pm 0.027) e^{i(0.18 \pm 0.26 \pm 0.02)}$

(a) Discriminating Variables: Mass, lifetime,  $\Delta\phi$  and isolation ( $p_t(\mu)$  divided by all  $p_t$  in a cone around the  $\mu$ ). (b) 1 event found in overlap of search windows - consistent with bkg estimate of  $1.05 \pm 0.30$  ( $B_d$ ),  $1.07 \pm 0.31$  ( $B_s$ ),  $1.75 \pm 0.34$  (combined). (c) Projected and current sensitivity to  $B_s \rightarrow \mu\mu$  at CDF, not including expected improvements due to increased  $\mu$  coverage.



to the measurement of two CP even amplitudes  $A_0$  and  $A_{\parallel}$ , and one CP-odd amplitude,  $A_{\perp}$ <sup>7</sup>. The CDF Run II results for  $192 \text{ pb}^{-1}$  are shown in Table 2, for both  $B_s \rightarrow J/\psi\phi$  and, as a cross check,  $B_d \rightarrow J/\psi K^{*0}$ . The  $B_d$  results are consistent with those from BaBar<sup>8</sup> and CLEO<sup>9</sup>. The phases of the amplitudes provide an interesting test of factorisation, which predicts the relative phases to be either 0 or  $\pi$ <sup>10</sup>. The amplitude measurements imply a CP-even content in  $B_s \rightarrow J/\psi\phi$  of  $77\% \pm 10\%$ . Work is in progress to combine this technique with the lifetime analysis for a  $\Delta\Gamma_s$  measurement.

#### 2.4 Search for New Physics with $B_{d,s} \rightarrow \mu^+\mu^-$

While in the Standard Model, the branching ratio of  $B_{d,s} \rightarrow \mu^+\mu^-$  is  $\mathcal{O}(10^{-9})$ , which is below the sensitivity of the Tevatron, many New Physics models predict enhancements of this mode by several orders of magnitude, for example mSUGRA<sup>11</sup> and SO(10) Symmetry Breaking models<sup>12</sup>. In mSUGRA, the  $B_{d,s} \rightarrow \mu^+\mu^-$  branching ratio is approximately<sup>11</sup>

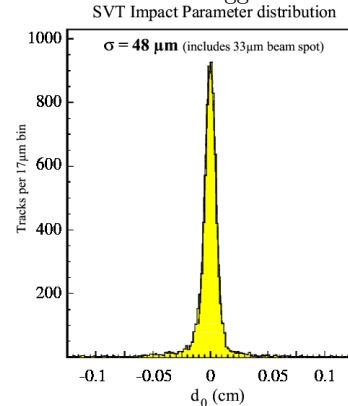
$$\text{BR}_{\text{mSUGRA}}(B_s \rightarrow \mu\mu) \approx 10^{-6} \cdot \tan^6 \beta \frac{M_{1/2}^2 \text{GeV}^4}{(M_{1/2}^2 + M_0^2)^3}$$

which increases rapidly with large  $\tan\beta$ .

The search for  $B_{d,s} \rightarrow \mu^+\mu^-$  was performed as a blind analysis. The cuts were optimised using Monte-Carlo generated signal events and background events from real data. Signal and background distributions for the most important cuts are shown in Figure 1 (a). After all cuts are applied,  $1.05 \pm 0.30$  background events are expected in the  $B_d$  mass window and  $1.07 \pm 0.31$

Figure 2: The CDF hadronic 2-Track-Trigger.  $\Delta\phi$  is the angle between the tracks in the transverse plane. IP is the 2-D impact parameter of each of the two tracks.  $L_{xy}$  is the decay length in the transverse plane. The table on the left lists the trigger requirements. The figure on the right shows the IP resolution at trigger level.

L1: 2 XFT tracks, $p_t > 2 \text{ GeV}$ , $\Delta\phi < 135^\circ$ , $p_{t1} + p_{t2} > 5.5 \text{ GeV}$ .	
L2:	
2-body:	Multi-body:
e.g. $B_d^0 \rightarrow \pi\pi$	e.g. $B_s^0 \rightarrow D_s\pi$
$100 \mu\text{m} < IP < 1 \text{ mm}$	$120 \mu\text{m} < IP < 1 \text{ mm}$
$20^\circ < \Delta\phi < 135^\circ$	$2^\circ < \Delta\phi < 90^\circ$
$L_{xy} > 200 \mu\text{m}$	$L_{xy} > 200 \mu\text{m}$
IP of B $< 140 \mu\text{m}$	–
L3: Same with refined tracks & mass cuts.	



$B_s$  mass window, both are 200 MeV wide, and overlap. The number of background events predicted for the combined mass window is  $1.75 \pm 0.34$ . Several cross checks in real data have been performed before unblinding, for example using wrong-sign di-muon events ( $\mu^+\mu^+$  and  $\mu^-\mu^-$ ), which yielded consistent results. The total number of events found after unblinding is 1 event in the overlap region of the two mass windows, as shown in Figure 1 (b), resulting in the following 90% confidence limits:

$$\text{BR}(B_d \rightarrow \mu^+\mu^-) < 1.5 \cdot 10^{-7} \text{ (90\%CL)} \quad \text{BR}(B_s \rightarrow \mu^+\mu^-) < 5.8 \cdot 10^{-7} \text{ (90\%CL)}$$

which is, for the  $B_d$ , similar to the results from BaBar and BELLE, and more than a factor of 3 better than the previous best limit for  $B_s \rightarrow \mu\mu$ , which was provided by CDF Run I. The projected performance as a function of integrated luminosity, ignoring future improvements due to the expected increase in muon coverage, is shown in Figure 1 (c).

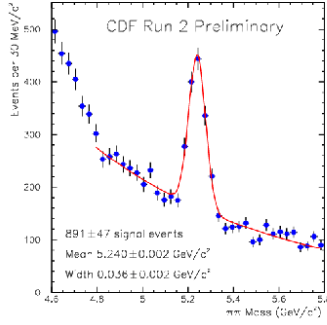
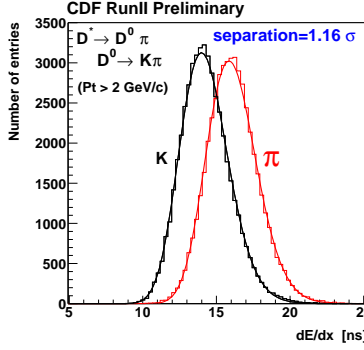
### 3 Results from the Impact Parameter-Based Hadronic B Trigger

#### 3.1 CDF's Two Track Trigger

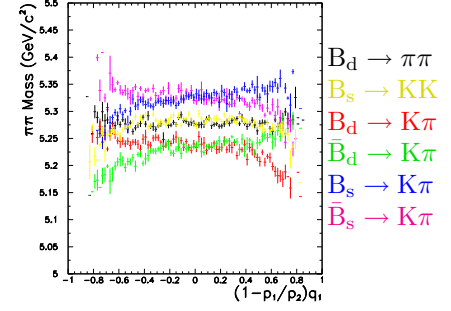
One of the most innovative improvements for B physics at CDF is the large-bandwidth hadron trigger, which triggers on the impact parameters of tracks at Level 2. The trigger requirements for the two scenarios, 2-body and multi-body B decays, are given in Figure 2. CDF's Two Track Trigger provides a unique sample of hadronic bottom and charm decays, that would otherwise be inaccessible, for example  $B^0 \rightarrow \pi\pi$  and  $B_s \rightarrow D_s\pi$ .

#### 3.2 $B \rightarrow hh$

Figure 3 (a) shows the invariant mass of reconstructed B to two-hadron events (assuming the hadrons are pions). About 900 events are found. In order to discriminate the different decay modes, pions and kaons are separated using their specific energy loss,  $\frac{dE}{dx}$ . The  $\pi/K$  discrimination using  $\frac{dE}{dx}$  has been measured using  $D^*$  decays and has been found to be  $1.16\sigma$ , as shown in figure 3 (b). Further discrimination between the different  $B \rightarrow hh$  decay modes is achieved using decay kinematics, as shown in 3 (c). The plot shows the reconstructed B mass in Monte Carlo simulated  $B \rightarrow hh$  events vs  $(1 - p_1/p_2) \cdot q_1$  for different decay modes. Here,  $p_1$  is the smaller of the two momenta,  $q_1$  is the charge of the particle with momentum  $p_1$ , and the mass is calculated assuming the decay products are pions. This led to the first observation of the decay

Figure 3:  $B \rightarrow hh$ (a) 891  $B \rightarrow hh$  in  $190 \text{ pb}^{-1}$ (b)  $K/\pi$  sep. from  $\frac{dE}{dx}$ 

(c) Kinematic variables (MC)



$B_s \rightarrow K^+K^-$ . A summary of the results from analysing  $B \rightarrow hh$  events in  $65 \text{ pb}^{-1}$  of data are given below:

- First observation of  $B_s \rightarrow KK$ :  $90 \pm 24$  out of 300  $B \rightarrow hh$  events.

- Search for  $CP$  in time-integrated rates

$$A_{CP} = \frac{\Gamma(\bar{B}_d^0 \rightarrow K^- \pi^+) - \Gamma(B_d^0 \rightarrow K^+ \pi^-)}{\Gamma(\bar{B}_d^0 \rightarrow K^- \pi^+) + \Gamma(B_d^0 \rightarrow K^+ \pi^-)} = 0.02 \pm 0.15 \pm 0.017$$

- Ratios of B.R.:

$$\frac{\Gamma(\bar{B}_d^0 \rightarrow \pi^+ \pi^-)}{\Gamma(\bar{B}_d^0 \rightarrow K^\pm \pi^\mp)} = 0.26 \pm 0.11 \pm 0.06, \quad \frac{\Gamma(B_s^0 \rightarrow K^+ K^-)}{\Gamma(B_s^0 \rightarrow K^\pm \pi^\mp)} = 2.71 \pm 0.73 \pm 0.35(f_s/f_d) \pm 0.81,$$

where  $(f_s/f_d)$  refers to the uncertainty due to the  $B_s/B_d$  production ratio.

Results for  $195 \text{ pb}^{-1}$  should follow, soon. In the long term, these methods can be used to extract the CP-violating phase  $\gamma$  from a combined analysis of time-dependent decay rate asymmetries in  $B_d \rightarrow \pi\pi$  and  $B_s \rightarrow KK$  <sup>13</sup>.

### 3.3 $D^0 \rightarrow hh$

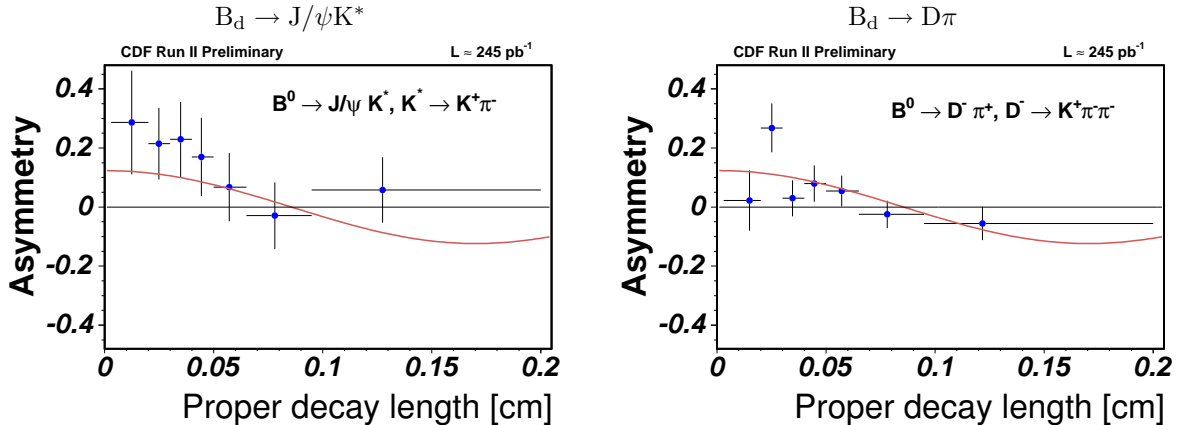
The Two Track Trigger also provides a huge charm signal, where the same methods can be applied. In the analysis presented here, only  $D^0$  mesons from  $D^*$  decays are used, which has two advantages: a very clean signal due to the highly effective cut on the difference between the reconstructed  $D^*$  and  $D^0$  mass, and the flavour of the  $D^0$  is known from the charge of the  $D^*$ . This allows a precise measurement of time-integrated CP asymmetries, which are expected to vanish in the Standard Model:

- $A_{CP KK} = \frac{\Gamma(\bar{D}^0 \rightarrow K^+ K^-) - \Gamma(D^0 \rightarrow K^+ K^-)}{\Gamma(\bar{D}^0 \rightarrow K^- K^+) + \Gamma(D^0 \rightarrow K^+ K^-)} = 2.0\% \pm 1.2\% \pm 0.6\%$
- $A_{CP \pi\pi} = \frac{\Gamma(\bar{D}^0 \rightarrow \pi^+ \pi^-) - \Gamma(D^0 \rightarrow \pi^+ \pi^-)}{\Gamma(\bar{D}^0 \rightarrow \pi^- \pi^+) + \Gamma(D^0 \rightarrow \pi^+ \pi^-)} = 1.0\% \pm 1.2\% \pm 0.6\%$

Branching ratios of  $D^0$  mesons are also of some interest, for example  $\frac{\Gamma(D^0 \rightarrow K^+ K^-)}{\Gamma(D^0 \rightarrow \pi^+ \pi^-)}$ , which is consistently larger experimentally, than theoretically predicted. The following summarises the ratios of B.R. results:

- $\frac{\Gamma(D^0 \rightarrow K^+ K^-)}{\Gamma(D^0 \rightarrow K^\pm \pi^\mp)} = 9.96\% \pm 0.11\% \pm 0.12\%$
- $\frac{\Gamma(D^0 \rightarrow \pi^+ \pi^-)}{\Gamma(D^0 \rightarrow K^\pm \pi^\mp)} = 3.608\% \pm 0.054\% \pm 0.12\%$
- $\frac{\Gamma(D^0 \rightarrow K^+ K^-)}{\Gamma(D^0 \rightarrow \pi^+ \pi^-)} = 2.762\% \pm 0.040\% \pm 0.034\%$

Figure 4: Time-dependent decay rate asymmetries for  $B_d$  mixing measurement, fitted simultaneously.



### 3.4 $B_s \rightarrow D_s \pi$

The decay of  $B_s$  to the flavour-eigenstate  $D_s \pi$  is the “flagship mode” for  $B_s$  mixing at CDF. Being fully reconstructible (no missing  $\nu$ ), it provides for excellent time resolution - in topologically similar decays, CDF currently achieves  $\sim 67$  fs, and hopes to improve once the innermost Si layer has been fully commissioned and aligned. In  $119 \text{ pb}^{-1}$ ,  $84 \pm 11$   $B_s \rightarrow D_s \pi$  have been reconstructed with a signal to background ratio of  $\sim 2$ . The reconstruction efficiency has been increased since data taking has started and is now at  $\sim 1.6$  events per  $\text{pb}^{-1}$ . These data can be used to calculate the relative production  $\times$  B.R. in  $B_s \rightarrow D_s \pi$  and  $B_d \rightarrow D \pi$ :

$$\frac{f_s \cdot BR(B_s^0 \rightarrow D_s^- \pi^+)}{f_d \cdot BR(B_d^0 \rightarrow D^- \pi^+)} = 0.35 \pm 0.05 \pm 0.04 \pm 0.09(BR)$$

where the last error is due to the uncertainty in the B.R. of the charm mesons.

### 3.5 $B_d$ mixing

A further step towards measuring  $B_s$  mixing is to make the somewhat easier measurement in the  $B_d$  system and check for consistency with the well-established results from the B factories, and Run 1. About  $1k$   $B_d \rightarrow J/\psi K^*$  and  $5k$   $B_d \rightarrow D \pi$  events from  $270 \text{ pb}^{-1}$  were used for this measurement. The mass difference is extracted by measuring the oscillation frequency in time-dependent decay rate asymmetries. The asymmetries are between B decays that did not change flavour (e.g.  $B^0 \rightarrow \bar{D}^0 \pi^-$ , neglecting Cabbibo suppressed decays), and those that did (e.g.  $B^0 \rightarrow D^0 \pi^+$ ). In the measurement presented here, the flavour of the  $B^0$  at birth was determined using same-side tagging only, which is based on the correlation of the  $B_d^0$  or  $\bar{B}_d^0$  flavour at birth, and the charge of the pion produced alongside, picking up the “left over”  $\bar{d}$  or  $d$  quark. (The same principle can be applied to  $B_s$  mesons, using Kaon tags.) The tagging efficiency and dilution are measured using charged B decays. The tagging power for same-side pion tagging is

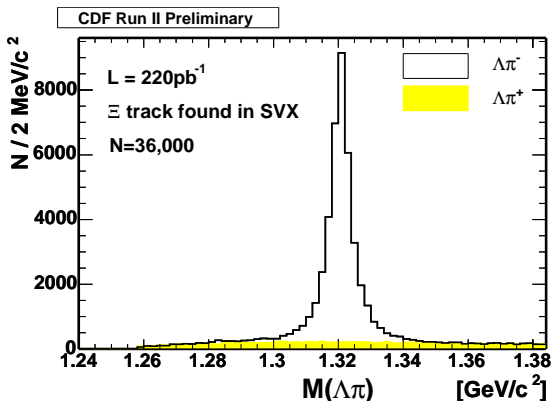
$$\varepsilon D^2 = (1.0 \pm 0.5 \pm 0.1) \%$$

where  $\varepsilon = (63 \pm 0.6)\%$  is the tagging efficiency (fraction of tagged events) and  $D = (12.4 \pm 3.3)\%$  the “dilution” defined as  $D \equiv (1 - 2\omega)$ , where  $\omega$  is the mis-tag fraction. Note that a large “dilution”, according to this definition, is a good thing. The tagging power  $\varepsilon D^2$  describes the statistical power of the tag:  $N$  events before tagging are statistically equivalent  $\varepsilon D^2 \times N$  perfectly tagged events. A simultaneous fit to the time-dependent decay rate asymmetries in  $B_d \rightarrow J/\psi K$  and  $B_d \rightarrow D \pi$ , shown in Figure 4 yields for the mass difference in the  $B_d$  system:

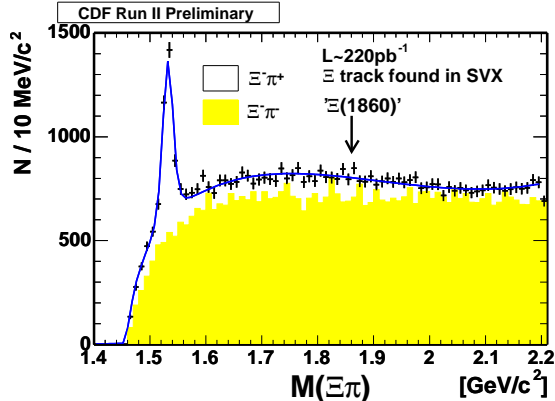
$$\Delta m_d = (0.55 \pm 0.10 \pm 0.01) \text{ ps}^{-1}$$

Figure 5: Searching for  $\Xi(1860)$ .

(a)  $\Xi^- \rightarrow \Lambda(p\pi)\pi^-$  reconstruction.



(b) Invariant mass  $M(\Xi^-, \pi^\pm)$ . The peak at 1530 MeV is the well-known  $\Xi^0(1530)$ .



**Opposite side tagging** In independent studies, other tagging methods have been investigated. Opposite side muon tagging yields a tagging power of  $\varepsilon D^2 = (0.660 \pm 0.093)\%$ , jet charge tagging  $\varepsilon D^2 = (0.419 \pm 0.024(stat))\%$ . Further taggers are under investigation.

### 3.6 Pentaquarks

The impact-parameter based trigger does not only provide large numbers of bottom and charm mesons, but of all long lived particles, including the  $\Xi^-$ . Combining this with a pion allows to search for the  $\Xi^0(1860)$  and  $\Xi^{--}$  observed at NA49<sup>1</sup>, which is often interpreted as a pentaquark.

CDF searches for the  $\Xi^0(1860)$  and  $\Xi^{--}$  in the decay modes  $\Xi^0(1860) \rightarrow \Xi^- \pi^+$  and  $\Xi^{--} \rightarrow \Xi^- \pi^-$  with  $\Xi^- \rightarrow \Lambda(p\pi)\pi^-$ . The  $\Xi^-$  lives long enough to leave hits in the Si detector before decaying. Requiring hits from the  $\Xi^-$  in the Si provides a very efficient cut. Figure 5 (a) shows the mass distribution a sample of 36,000  $\Xi^-$ . The tiny background contribution, estimated from wrong-charge combinations, is superimposed as the shaded histogram.

In a second step, the  $\Xi^-$  is combined with a  $\pi^\pm$ . Figure 5 (b) shows the invariant mass distribution for same charge (shaded histogram) and opposite charge (black crosses) combinations of  $\Xi^-$  and pions. The line represents a fit to the opposite charge mass distribution. There is a clear peak at the well-known  $\Xi^0(1530)$  resonance, that is used as a reference in this analysis. However, neither the same sign nor the opposite sign combination show any evidence of a resonance at 1860 MeV. As a cross check, the analysis was repeated using the Jet20 trigger sample, that is not affected by an impact parameter cut. For  $4k$   $\Xi^-$  in the Jet20 sample, no evidence of a  $\Xi(1860)$  was found. The 95% upper confidence limits for the *ratio* of  $\Xi(1860)$  to the known  $\Xi^0(1530)$  are:

$\Xi^- \pi^+$ (search) / $\Xi(1530)$ (control)	0.07
$\Xi^- \pi^-$ (search) / $\Xi(1530)$ (control)	0.04

## 4 Conclusion

Large numbers of B hadrons of all flavours are produced at the Tevatron. CDF has measured the  $b$  production cross section in  $b \rightarrow J/\psi X$  events. Fully reconstructed  $B \rightarrow J/\psi X$  events have been used for precise lifetime measurements of  $B_d, B_s$  and  $\Lambda_b$  hadrons, which will provide a test of Heavy Quark Expansion. The CP content of  $B_s \rightarrow J/\psi \phi$  has been measured using a transversity angle analysis, which will be combined with the lifetime measurement to extract  $\Delta\Gamma_s$ . Data from

the leptonic B trigger were also used to obtain the best current limit on the B.R. of  $B_s \rightarrow \mu\mu$ , one of the most sensitive probes of new physics at the Tevatron.

CDF's high bandwidth Two Track Trigger provides a unique sample of hadronic B and Charm decays, including  $B \rightarrow hh$ , which led to the first observation of  $B_s \rightarrow KK$ , and will be used for CP violation studies as more data become available. First steps towards a  $B_s$  mixing measurement have been taken with the reconstruction of  $B_s \rightarrow D_s\pi$  events, and mixing measurements in the  $B_d$  system.

The huge sample of  $\Xi^-$  found in the Two Track Trigger has been used for a sensitive search for  $\Xi(1860)$ , which was not found. The B triggers will be used for many more pentaquark searches, especially those decaying to  $J/\psi$  or D and baryons.

## References

1. C. Alt *et al.* [NA49 Collaboration], Phys. Rev. Lett. **92**, 042003 (2004) [arXiv:hep-ex/0310014].
2. N. Uraltsev, [arXiv:hep-ph/9804275].
3. M. A. Shifman, [arXiv:hep-ph/0009131].
4. Heavy Flavour Averaging Group. Method:  
D. Abbaneo *et al.* [ALEPH, CDF, DELPHI, L3, OPAL, SLD], June 2001, CERN-EP/2001-050, [arXiv:hep-ex/0112028]. Results for PDG-2004: [http://www.slac.stanford.edu/xorg/hfag/osc/PDG\\_2004/index.html](http://www.slac.stanford.edu/xorg/hfag/osc/PDG_2004/index.html) Results for PDG-2002: [http://lepboosc.web.cern.ch/LEPBOSC/combined\\_results/PDG\\_2002/](http://lepboosc.web.cern.ch/LEPBOSC/combined_results/PDG_2002/)
5. F. Abe *et al.* [CDF] Phys. Rev. D **57** (1998) 5382 Phys. Rev. **D57**, 5382; Phys. Rev. Lett. **76**, (1996) 4462; Phys. Rev. D **58** (1998) 092002; Phys. Rev. Lett. **77**, (1996) 1945; Phys. Rev. D **57**, (1998) 5382; Phys. Rev. Lett. **77** (1996) 1439; See also: [http://www-cdf.fnal.gov/physics/new/bottom/blife\\_summary/blife\\_summary.html](http://www-cdf.fnal.gov/physics/new/bottom/blife_summary/blife_summary.html)
6. M Battaglia, AJ Buras, P Gambino and A Stocchi, eds. Proceedings of the *First Workshop on the CKM Unitarity Triangle*, CERN, Feb 2002, [arXiv:hep-ph/0304132].
7. A. S. Dighe, I. Dunietz, H. J. Lipkin and J. L. Rosner, Phys. Lett. B **369**, 144 (1996) [arXiv:hep-ph/9511363].
8. B. Aubert *et al.* [BABAR Collaboration], Phys. Rev. Lett. **87** (2001) 241801 [arXiv:hep-ex/0107049].
9. C. P. Jessop *et al.* [CLEO Collaboration], Phys. Rev. Lett. **79** (1997) 4533 [arXiv:hep-ex/9702013].
10. T. W. Yeh and H. n. Li, Phys. Rev. D **56** (1997) 1615 [arXiv:hep-ph/9701233].
11. A. Dedes, H. K. Dreiner and U. Nierste, Phys. Rev. Lett. **87** (2001) 251804 [arXiv:hep-ph/0108037].
12. R. Dermisek, S. Raby, L. Roszkowski and R. Ruiz De Austri, JHEP **0304** (2003) 037 [arXiv:hep-ph/0304101].
13. R. Fleischer, Phys. Lett. B **459** (1999) 306 [arXiv:hep-ph/9903456].